International Journal of Mathematical Archive-3(7), 2012, 2495-2515
Available online through www.ijma.info ISSN 2229 – 5046

CONVECTIVE FLOW AND HEAT TRANSFER BETWEEN WAVY WALL AND A PARALLEL FLAT WALL DIVIDED BY A PERFECTLY CONDUCTIVE BAFFLE

J. C. Umavathi*
Professor in Department of Mathematics, Gulbarga University, Gulbarga-585 106, Karnataka, India

(Received on: 20-06-12; Accepted on: 10-07-12)

ABSTRACT

The steady two-dimensional free convection flow of a viscous fluid in a vertical double passage wavy channel has been investigated analytically. The channel is divided into two passages by means of a thin, perfectly conductive plane baffle and the velocity and temperature will be individual in each streams. The governing equations of the fluid and the heat transfer have been solved subject to the relevant boundary conditions by assuming that the solution consists of two parts; a mean part and disturbance or perturbed part. To obtain the perturbed part of the solution, the long wave approximation has been used and to solve the mean part, well known approximation used by Ostrach [1] has been utilized. Results are presented graphically for the distribution of velocity and temperature fields for varying physical parameters such as baffle position, Grashof number, wall temperature ratio and product of non-dimensional wave number and space-coordinate at different positions of the baffle. The relevant flow and heat transfer characteristics namely, skin friction and the rate of heat transfer at both the walls has been discussed in detail.

Keywords: *Wavy vertical channel, baffle, viscous fluid*

1. INTRODUCTION

Natural convection in vertical channels and tubes has been studied extensively because of its interest in many practical systems, including cooling of electronic equipment [2, 3], chimneys and furnaces, heat exchangers and solar energy collectors, nuclear engineering and geo-physical flows. Early experiments were carried out by Elenbaas [4] and Ostroumove [5] and later by Sparrow and Bahrami [6], for isothermal tubes and plates heated at temperatures above the ambient temperature. Bodoia and Osterle [7] analyzed the flow in a vertical channel with uniform wall temperature; Engel and Muller [8] applied an integral method to channels of infinite height with uniform wall temperature or uniform surface heat flux.

When the channel is divided into several passages by means of plane baffles, as usually occurs in heat exchangers or electronic equipment, it is quite possible to enhance the heat transfer performance between the walls and fluid by the adjustments of each baffle position and strengths of the separate flow streams. In such configurations, perfectly conductive and thin baffles may be used to ovoid significant increase of the transverse thermal resistance. Stronger streams may be arranged to occur within the passages near the channel wall surfaces in order to cool or heat the walls more effectively. Even though the subject of channel flow has been investigated extensively, few studies have so far evaluated for these effects. It is necessary to study the heat and mass transfer from an irregular surface because irregular surfaces are often present in many applications. It is often encountered in heat transfer devices to enhance the heat transfer. Mixed convection from irregular surfaces can be used for transferring heat in several heat transfer devices. For example, flat-plate, solar collectors and flat-plate condensers in refrigerators. The natural convection heat transfer from an isothermal vertical wavy surface was first studied by Yao [9, 10], and using an extended Prandtl's transposition theorem and a finite difference scheme. He proposed a simple transformation to study the natural convection heat transfer from isothermal vertical wavy surfaces, such as sinusoidal surface. Moulic and Yao [11] solved for mixed convection with thermal diffusion. Along a vertical wavy surface, Chiu and Chou [12] studied the natural convection heat transfer in micropolar fluids. Chen and Wang [13] analyzed transient free convection along a wavy surface in microfluids. Malashetty et al. [14] studied on magneto-convective flow and heat transfer between vertical wavy wall and a parallel flat wall. Umavathi et al. [15-17] also studied two fluid flow in a vertical wavy channel.

Corresponding author: *J. C. Umavathi**
Professor in Department of Mathematics, Gulbarga University, Gulbarga-585 106, Karnataka, India

Das and Mahmud [18] analyzed the free convection inside both the bottom and the ceiling wavy and isothermal enclosure. They indicated that, only at the lower Grashof number, the heat transfer rate rises when the amplitude wavelength ratio changes from zero to other values. Recently, Dalal and Das [19] made a numerical solution to investigate the inclined right wall wavy enclosure with spatially variable temperature boundary conditions. Oztop [20] applied the electric grid generation and obtained sinusoidal duct geometry to enhance the forced convection heat transfer. Varol and Oztop [21] investigated the effects of inclination angle on the laminar natural convection heat transfer and fluid flow in a wavy solar collector in steady state regime. They observed that the inclination angle is the most important and effective parameter on heat transfer which can be used to control the heat transfer inside the collector.

Most of the previous studies about vertical wavy surfaces are concerned with micro fluids or porous media. Recently, Jang et al. [22], has studied numerically on natural convection heat and mass transfer along a vertical wavy surface. Yet the preceding literature survey shows that mixed convection heat and mass transfer in Newtonian fluid along a vertical wavy surface has not been well investigated. The flow and thermal field in an isothermal vertical wavy enclosure was studied by Mahmud et al. [23] for Grashof number and orientations. Khalil et al. [24] analyzed the natural convection heat transfer in a wavy porous enclosure using non-Darcian model. They found that the amplitude of the wavy surface and the number of undulation affected the heat transfer characteristics. Hasnaoui et al. [25], Ben-Nakhi and Camkha [26], Dagtekin and Oztop [27] investigated also the natural convection in enclosures with a partition. The presence of a partition was the effective parameter on heat transfer. Tansmim and Collins [28] did a numerical study on heat transfer in a square cavity with a baffle located on the hot wall. The study showed that the baffle has a significant effect on increasing the rate of heat transfer compared with a wall without baffle. Recently Prathap Kumar et al. [29, 30] analyzed free convection in a double passage wavy channel using Walters Fluid. Cheng and Shiau [31] studied the effects of a horizontal baffle on the heat transfer characteristics of pulsating opposing mixed convection in a parallel vertical open channel. The influences of the dimensionless pulsating frequency, Strouhal number and magnitude, Prandtl number and baffle position on the velocity and temperature distribution and long time average Nusselt number variation for the system at various Reynolds number and square of mixed convection parameter were explored in detail. The result showed that the channel with both flow pulsation and a baffle gives the best heat transfer.

Heat transfer enhancement in a heat exchanger tube by installing a baffle was reported by Nasiruddin and Siddiqui [32]. The effect of baffle size and orientation on the heat transfer enhancement was studied in detail. Three different baffle arrangements were considered. The results showed that for the vertical baffle, an increase in the baffle height cause a substantial increase in the Nusselt number but the pressure loss is also very significant. For the inclined baffles, the result show that the Nusselt number enhancement is almost independent of baffle inclination angle, with the maximum and average Nusselt number was 120% and 70% higher than that for the case of no baffle, respectively. For a given baffle geometry, the Nusselt number enhancement was increased by more than a factor of two as the Reynolds number decreased from 20,000 to 5000. Simulations were conducted by introducing another baffle to enhance heat transfer. The result show that the average Nusselt number for the two baffles case is 20% higher than the one baffle case and 82% higher than the no baffle case. The above results suggest that a significant heat transfer enhancement in a heat exchanger tube can be achieved by introducing a baffle inclined towards downstream side with the minimum pressure loss. Mixed convection heat transfer in an inclined parallel-plate channel with a transverse fin located at lower channel wall was investigated numerically by Yang et al. [33].

Keeping the interest of heat transfer problems owing to their practical applications, an attempt is made to understand the flow and heat transfer in a vertical wavy channel by introducing a perfectly thin baffle.

2. MATHEMATICAL FORMULATION

Consider a steady, two-dimensional laminar fully developed free convection flow in an open ended vertical channel filled with purely viscous fluid. The geometry under consideration illustrated in Figure 1 consists of wavy wall situated at $Y = \varepsilon^* \cos(kX)$ and flat wall at $Y = d$. The X-axis is taken vertically upward, and parallel to the direction of buoyancy, and the Y-axis is normal to it. The wavy and flat walls are maintained at a constant temperature T_w and T_1, respectively. The fluid properties are assumed to be constant and the Boussinesq approximation will be used so that the density variation is retained only in the buoyancy term. Further it is also assumed that the wavelength of the wavy wall is large compared with the breadth of the channel. The channel is divided into two passages by means of a perfectly conducting thin baffle, for which the transverse thermal resistance can be neglected (Cheng et al. [34] and Salah El Din [35, 36]).

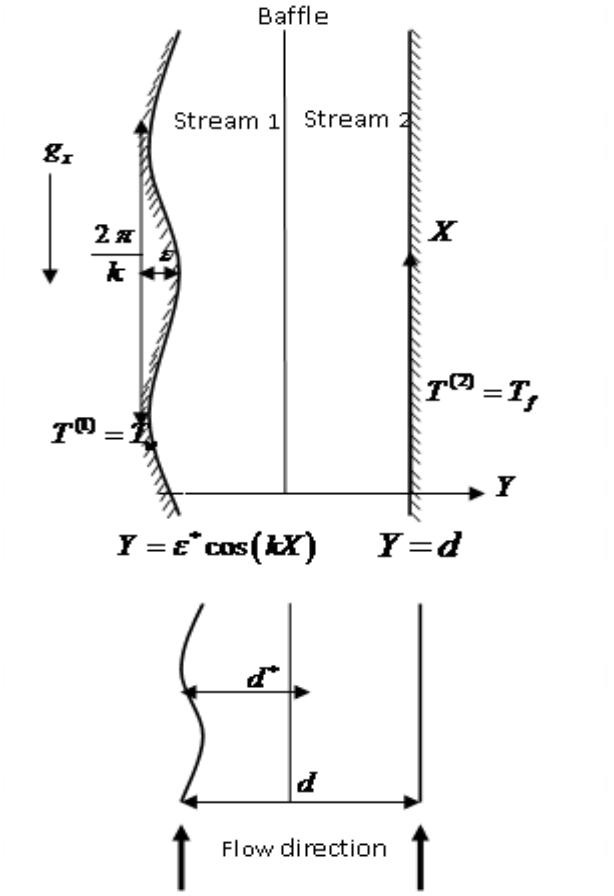

Fig. 1: Physical configuration of the double-passage channel

Introducing the following non-dimensional variables in the governing equations for velocity and temperature as,

$$x = \frac{X}{d},\ y = \frac{Y}{d},\ u_i = \frac{U_i d}{\nu},\ v_i = \frac{V_i d}{\nu},\ \theta = \frac{T - T_s}{T_w - T_s},\ \overline{p} = \frac{p^*}{\rho\left(\nu/d\right)^2} \tag{1}$$

Doing this, one obtains the equation of continuity as

$$\frac{\partial u_i}{\partial x} + \frac{\partial v_i}{\partial y} = 0 \tag{2}$$

and the momentum equation becomes

$$\left(u_i \frac{\partial u_i}{\partial x} + v_i \frac{\partial u_i}{\partial y}\right) = -\frac{\partial \overline{P_i}}{\partial x} + \frac{\partial^2 u_i}{\partial x^2} + \frac{\partial^2 u_i}{\partial y^2} + G\theta_i \tag{3}$$

$$\left(u_i \frac{\partial v_i}{\partial x} + v_i \frac{\partial v_i}{\partial y}\right) = -\frac{\partial \overline{P_i}}{\partial y} + \frac{\partial^2 v_i}{\partial x^2} + \frac{\partial^2 v_i}{\partial y^2} \tag{4}$$

The energy equation becomes

$$P\left(u_i \frac{\partial \theta_i}{\partial x} + v_i \frac{\partial \theta_i}{\partial y}\right) = \frac{\partial^2 \theta_i}{\partial x^2} + \frac{\partial^2 \theta_i}{\partial y^2} \tag{5}$$

Subject to the boundary conditions,

$$\begin{aligned} &u_1 = v_1 = 0, \theta_1 = 1 \qquad \text{on } y = \varepsilon\cos(\lambda x) \\ &u_1 = u_2 = 0,\ v_1 = v_2 = 0, \text{ on } y = y^* \\ &\theta_1 = \theta_2,\ \frac{\partial\theta_1}{\partial y} + \frac{\partial\theta_1}{\partial x} = \frac{\partial\theta_2}{\partial y} + \frac{\partial\theta_2}{\partial x} \text{ on } y = y^* \\ &u_2 = v_2 = 0, \qquad \theta_2 = m \qquad \text{on } y = 1 \end{aligned} \tag{6}$$

where $P = \mu c_p / k$, the Prandtl number, $\varepsilon = \varepsilon^* / d$, the dimensionless amplitude parameter, $\lambda = kd$, the dimensionless frequency parameter, $m = (T_1 - T_s)/(T_w - T_s)$, the wall temperature ratio and $G = d^3 g_x \beta (T_w - T_s)/\nu^2$, the Grashof number. The subscript s denotes quantities in the static fluid condition.

3. SOLUTIONS

Equations (3) to (5) are coupled non-linear partial differential equations and hence finding exact solutions is out of scope. However, for small values of the amplitude parameter ε, approximate solutions can be extracted through the perturbation method. The amplitude parameter ε is usually small and hence regular perturbation method can be strongly justified. Adopting this technique, solutions for velocity and temperature are assumed in the form

$$\begin{aligned} &u_i(x,y) = u_{i0}(y) + \varepsilon u_{i1}(x,y)\ ,\ v_i(x,y) = \varepsilon v_{i1}(x,y) \\ &\overline{p}_i = p_{i0}(x) + \varepsilon p_{i1}(x,y)\ ,\quad \theta_i(x,y) = \theta_{i0}(y) + \varepsilon\theta_{i1}(x,y) \end{aligned} \tag{7}$$

where the perturbations u_{i1}, v_{i1}, p_{i1} and θ_{i1} are small compared with the mean or zeroth order quantities. Equations (2) to (6) yield the following equations.
Zeroth order equations

$$\frac{d^2 u_{i0}}{dy^2} + G\theta_{i0} = 0\,;\ \frac{d^2\theta_{i0}}{dy^2} = 0 \tag{8}$$

First order equations

$$\frac{\partial u_{i1}}{\partial x} + \frac{\partial v_{i1}}{\partial y} = 0 \tag{9}$$

$$u_{i0}\frac{\partial u_{i1}}{\partial x} + v_{i1}\frac{\partial u_{i0}}{\partial y} = -\frac{\partial\overline{P_{i1}}}{\partial x} + \frac{\partial^2 u_{i1}}{\partial x^2} + \frac{\partial^2 u_{i1}}{\partial y^2} + G\theta_{i1} \tag{10}$$

$$u_{i0}\frac{\partial v_{i1}}{\partial x} = -\frac{\partial\overline{P_{i1}}}{\partial y} + \frac{\partial^2 v_{i1}}{\partial x^2} + \frac{\partial^2 v_{i1}}{\partial y^2} \tag{11}$$

$$P\left(u_{i0}\frac{\partial\theta_{i1}}{\partial x} + v_{i1}\frac{d\theta_{i0}}{dy}\right) = \frac{\partial^2\theta_{i1}}{\partial x^2} + \frac{\partial^2\theta_{i1}}{\partial y^2} \tag{12}$$

In deriving the equation (8), the constant pressure gradient term $\frac{\partial}{\partial x}(p_0 - p_s)$ has been taken equal to zero following Ostrach [1]. In view of equation (7) the boundary condition in equation (6) can be split up into the following two parts.

Zeroth order boundary conditions

$$\begin{aligned} &u_{10} = 0, \qquad \theta_{10} = 1 \qquad \text{on } y = 0 \\ &u_{10} = u_{20} = 0,\ \theta_{10} = \theta_{20},\ \frac{d\theta_{10}}{dy} = \frac{d\theta_{20}}{dy} \text{ on } y = y^* \\ &u_{20} = 0,\ \theta_{20} = m \text{ on } \qquad y = 1 \end{aligned} \tag{13}$$

First order boundary conditions

$$u_{11} = -rp\left(e^{i\lambda x}\frac{du_{10}}{dy}\right), \qquad v_{11} = 0, \;\; \theta_{11} = -rp\left(e^{i\lambda x}\frac{d\theta_{10}}{dy}\right) \;\; \text{on} \;\; y = 0$$

$$u_{11} = u_{21} = 0, \;\; v_{11} = v_{21} = 0, \; \theta_{11} = \theta_{21}, \; \text{on} \;\; y = y^* \tag{14}$$

$$u_{21} = 0, \;\; v_{21} = 0, \;\; \theta_{21} = 0, \;\; \text{on} \;\; y = 1$$

where rp represents the real part

The solutions for zeroth order velocity u_{i0} and zeroth order temperature θ_{i0} satisfying the equation (8) and the boundary conditions (13) are given by

Stream 1:

$$\theta_{10} = c_1 y + c_2 \tag{15}$$

$$u_{10} = l_1 y^3 + l_2 y^2 + d_1 y + d_2 \tag{16}$$

Stream 2:

$$\theta_{20} = c_7 y + c_8 \tag{17}$$

$$u_{20} = l_6 y^3 + l_7 y^2 + d_{11} y + d_{12} \tag{18}$$

In order to solve equations (9) to (12) for the first order quantity it is convenient to introduce stream function $\bar{\psi}$ in the following form

$$u_{i1} = -\frac{\partial \bar{\psi}_{i1}}{\partial y}, \;\; v_{i1} = \frac{\partial \bar{\psi}_{i1}}{\partial x} \;\; \text{for} \;\; i = 1, 2 \tag{19}$$

The stream function approach reduces the number of dependent variables to be solved and also eliminates pressure from the list of variables. Differentiate equation (10) with respect to y and differentiate equation (11) with respect to x and then subtract equation (10) with equation (11) which will result in the elimination of pressure p_{i1}. We assume stream function and temperature in the following form

$$\bar{\psi}_{i1}(x, y) = e^{i\lambda x}\psi_{i1}(y), \qquad \theta_{i1}(x, y) = e^{i\lambda x}t_{i1}(y)$$

From the above, equations (9) to (12) after elimination of p_{i1}, can be expressed in terms of the stream function ψ and t in the form

$$\psi_i^{iv} - \psi_i^{''}\left(2\lambda^2 + i\lambda u_{i0}\right) + \psi_i\left(\lambda^4 + i\lambda u_{i0}^{''} + i u_{i0}\lambda^3\right) = Gt_i^{'} \tag{20}$$

$$t_i^{''} - \lambda^2 t_i = P\,\mathrm{i}\,\lambda\left(u_{10}t_i + \psi_i\theta_{i0}^{'}\right) \tag{21}$$

where i is the coefficient of imaginary part and suffix i = 1,2 denotes stream-1 and stream-2 respectively.

Boundary conditions as defined in equation (14) can be written in terms of ψ and t as

$$\psi_1^{'} = u_{10}^{'}, \psi_1 = 0, \;\; t_1 = -\theta_{10}^{'} \text{ on } y = 0$$

$$\psi_1^{'} = 0, \;\; \psi_1 = 0, \;\; \psi_2^{'} = 0, \;\; \psi_2 = 0, \;\; \text{on } y = y^* \tag{22}$$

$$t_1 = t_2, \;\; t_1^{'} = t_2^{'}, \;\; \text{on } y = y^*$$

$$\psi_2^{'} = 0, \;\; \psi_2 = 0, \;\; t_2 = 0, \text{on } y = 1$$

We restrict our attention to the real parts of the solutions for the perturbed quantities ψ , t , u_{i1} and v_{i1} .

Consider only small values of λ . On substituting

$$\psi(\lambda, y) = \sum_{r=0}^{\infty} \lambda^r \psi_r , \quad t(\lambda, y) = \sum_{r=0}^{\infty} \lambda^r t_r \tag{23}$$

into equations (20) to (22) we obtain to the order of λ , the following set of ordinary differential equations Zeroth order

$$t_{i0}^{''} = 0 \tag{24}$$

$$\psi_{i0}^{iv} = G t_{i0}^{'} \tag{25}$$

First order

$$t_{i1}^{''} = P\,\mathrm{i}\left(u_{i0} t_{i0} + \psi_{i0} \theta_{10}^{'}\right) \tag{26}$$

$$\psi_{i1}^{iv} = i u_{i0} \psi_{i0}^{''} - i u_{i0}^{''} \psi_{i0} + \mathrm{i}\,K\left(u_{i0} \psi_{i0}^{iv} - u_{i0}^{iv} \psi_{1}\right) + G t_{i1}^{'} \tag{27}$$

Zeroth order boundary conditions in terms of stream function and temperature are

$$\begin{aligned}
&\psi_{10}^{'} = u_{10}^{'}, \quad \psi_{10} = 0, \; t_{10} = -\theta_{10}^{'} \quad \text{on} \; y = 0 \\
&\psi_{10}^{'} = 0, \; \psi_{10} = 0, \; \psi_{20}^{'} = 0, \; \psi_{20} = 0, \; \text{on} \quad y = y^{*} \\
&t_{10} = t_{20}, \; t_{10}^{'} = t_{20}^{'}, \; \text{on} \quad y = y^{*} \\
&\psi_{20}^{'} = 0, \; \psi_{20} = 0, \; t_{20} = 0, \; \text{on} \quad y = 1
\end{aligned} \tag{28}$$

First order boundary conditions in terms of stream function and temperature are

$$\begin{aligned}
&\psi_{11}^{'} = 0, \; \psi_{11} = 0, \; t_{11} = 0 \quad \text{on} \quad y = 0 \\
&\psi_{11}^{'} = 0, \; \psi_{11} = 0, \; \psi_{21}^{'} = 0, \; \psi_{21} = 0, \; \text{on} \; y = y^{*} \\
&t_{11} = t_{21}, \; t_{11}^{'} = t_{21}^{'}, \; \text{on} \; y = y^{*} \\
&\psi_{21}^{'} = 0, \; \psi_{21} = 0, \; t_{21} = 0, \; \text{on} \quad y = 1
\end{aligned} \tag{29}$$

The set of equations (24) to (27) subject to boundary conditions as given in equations (28) and (29) have been solved exactly for ψ and t . From these solutions, the first order quantities can be put in the form,

$$\psi = \left(\psi_{rp} + \mathrm{i}\,\psi_{\mathrm{i}\,p}\right) = \psi_{i0} + \lambda \psi_{i1}, \quad t = \left(t_{rp} + \mathrm{i}\,t_{\mathrm{i}\,p}\right)_j = t_{i0} + \lambda t_{i1} \tag{30}$$

where suffix rp denotes the real part and $\mathrm{i}\,p$ denotes the imaginary part. Considering only the real part, the expression for first order velocity and temperature become

$$u_{i1} = -\cos(\lambda x)\psi_{i0}^{'} + \lambda \psi_{i1}^{'} \sin(\lambda x) \tag{31}$$

$$v_{i1} = -\lambda^2 \cos(\lambda x)\psi_{i1} - \lambda \psi_{i0} \sin(\lambda x) \tag{32}$$

$$\theta_{i1} = \cos(\lambda x)(t_{i0}) - \lambda t_{i1} \sin(\lambda x) \tag{33}$$

The first order and total solutions are given in Appendix.

3.1. Skin friction and Nusselt number

The shearing stress σ_{xy} at any point in the fluid in non-dimensional form is given by

$$\sigma_{xy} = \frac{d^2 \overline{\sigma}_{xy}}{\rho \nu^2} = u_0^{'}(y) + \varepsilon e^{i\lambda x} \overline{u}_1^{'}(y) + \mathrm{i}\,\varepsilon \lambda e^{i\lambda x} \overline{v}_1(y) \tag{34}$$

At the wavy wall, $y = \varepsilon \cos(\lambda x)$ skin friction takes the form

$$\sigma_w = \sigma_0^0(0) + \varepsilon\left(u_{10}^{"}\cos(\lambda x) + \lambda\psi_{11}^{"}(0)\sin(\lambda x) - \psi_{10}^{"}(0)\cos(\lambda x)\right) \tag{35}$$

and at the flat wall, $y = 1$ skin friction takes the form

$$\sigma_f = \sigma_1^0(0) + \varepsilon\left(-\psi_{20}^{"}(1)\cos(\lambda x) + \lambda\psi_{21}^{"}(1)\sin(\lambda x)\right) \tag{36}$$

where $\sigma_0^0(0) = \left(\frac{du_{10}}{dy}\right)_{y=0}$ and $\sigma_1^0(1) = \left(\frac{du_{20}}{dy}\right)_{y=1}$ are the zeroth order skin-friction at the walls.

The non-dimensional heat transfer coefficient known as Nusselt number (Nu) is given by

$$Nu = \frac{\partial\theta}{\partial y} = \theta_0'(y) + \varepsilon\,\mathrm{Re}\left(e^{i\lambda x}\theta_1'(y)\right) \tag{37}$$

At the wavy wall $y = -1 + \varepsilon\cos(\lambda x)$ Nusselt number Nu_w takes the form

$$Nu_w = Nu_0^0(0) + \varepsilon\left(\theta_{10}'(0)\cos(\lambda x) + t_{10}'(0)\cos(\lambda x) - \lambda t_{11}'(0)\sin(\lambda x)\right), \tag{38}$$

and at the flat wall $y = 1$,

$$Nu_f = Nu_1^0(1) + \varepsilon\left(t_{20}'(1)\cos(\lambda x) - \lambda t_{21}'(1)\sin(\lambda x)\right) \tag{39}$$

where $Nu_0^0(0) = \left(\frac{d\theta_{10}}{dy}\right)_{y=0}$ and $Nu_1^0(1) = \left(\frac{d\theta_{20}}{dy}\right)_{y=1}$ are zeroth order Nusselt number at the walls.

Velocity and temperature solutions are numerically evaluated for several sets of values of the governing parameters. Also, the wall skin friction σ_w, σ_f and the wall Nusselt number Nu_w, Nu_f are calculated numerically and some of the qualitative interesting features are presented.

3.2 Comparison of the Solutions with Salah El Din [36] in the presence of baffle

To validate the results of the present model, the problem is solved in the absence of the product of non-dimensional wave number and space co-ordinate and pressure gradient.. The dimensionless basic equations (2) to (5) become

$$\frac{d^2\theta_{i0}}{dy^2} = 0 \tag{40}$$

$$\frac{d^2u_{j0}}{dy^2} + G\theta_{j0} = 0 \tag{41}$$

To compare the results, the boundary conditions on temperature are taken as in Salah El Din [36], i.e.,

$$\theta_1 = -\frac{1}{2} \quad \text{on} \quad y = 0; \quad \theta_2 = \frac{1}{2} \quad \text{on} \quad y = 1$$
$$\theta_1 = \theta_2, \ \frac{d\theta_1}{dy} = \frac{d\theta_2}{dy} \text{ on } y = y^* \tag{42}$$

The boundary conditions on velocity are no-slip conditions on the boundary and vanishing of velocity at the baffle. That is

$$u_1 = 0 \quad \text{on} \quad y = 0; \quad u_2 = 0 \quad \text{on} \quad y = 1$$
$$u_1 = u_2 = 0 \text{ on } y = y^* \tag{43}$$

The solutions of equations (40) and (41) using boundary conditions (42) and (43) become

$$\theta_1 = y - \frac{1}{2}, \quad u_1 = -\frac{G}{2}\left(\frac{y^3}{3} - \frac{y^2}{2}\right) + d_1 y + d_2 \tag{44}$$

$$\theta_2 = y - \frac{1}{2}, \quad u_2 = -\frac{G}{2}\left(\frac{y^3}{3} - \frac{y^2}{2}\right) + d_3 y + d_4 \tag{45}$$

The above solutions agree very well with the solutions of Salah El Din [36].

3.3 Comparison of the Solutions with Rita and Alok [37] in the absence of baffle

The above case validates the results for flat wall. To validate the results for wavy wall, the problem is solved in the absence of the baffle and visco-elastic parameter and compared the results with Rita and Alok [37]. The comparison of the present model is carried out in two ways,

1. Shifting the baffle to the right wall and comparing the solutions of stream-1 with Rita and Alok [37].

The boundary conditions for this case become

$$\theta_{10} = 1, \; u_{10} = 0, \; t_{10} = -\theta_{10}', \; \psi_{10}' = u_{10}', \; \psi_{10} = 0, \quad \text{on} \quad y = 0$$
$$\theta_{10} = m, \; u_{10} = 0, \; t_{10} = 0, \; \psi_{10}' = 0, \; \psi_{10} = 0, \qquad \text{on} \quad y = 1 \tag{46}$$

$$t_{11} = 0, \; \psi_{11}' = 0, \; \psi_{11} = 0, \; \text{on} \quad y = 0$$
$$t_{11} = 0, \; \psi_{11}' = 0, \; \psi_{11} = 0 \qquad \text{on} \quad y = 1 \tag{47}$$

The solution of stream-1 with above boundary conditions become

$$\theta_{10} = c_1 y + c_2; \qquad u_{10} = l_1 y^3 + l_2 y^2 + d_1 y + d_2 \tag{48}$$

$$t_{10} = c_3 y + c_4; \qquad \psi_{10} = l_3 y^4 + \frac{d_3}{6} y^3 + \frac{d_4}{2} y^2 + d_5 y + d_6 \tag{49}$$

$$t_1 = Pi\left(m_1 y^6 + m_2 y^5 + m_3 y^4 + m_4 y^3 + m_5 y^2\right) + c_5 y + c_6,$$
$$\psi_{11} = i\left(\frac{n_1}{3024} y^9 + \frac{n_2}{1680} y^8 + \frac{n_3}{840} y^7 + \frac{n_4}{360} y^6 + \frac{n_5}{120} y^5 + \frac{n_6}{24} y^4\right) + \frac{n_7}{24} y^4 + \frac{d_7}{6} y^3 + \frac{d_8}{2} y^2 + d_9 y + d_{10} \tag{50}$$

With the above solutions the velocity and temperature field become

$$u_1 = u_{10} + \varepsilon\left(-\cos(\lambda x)\psi_{10}' + \lambda\psi_{11}' \sin(\lambda x)\right) \tag{51}$$

$$v_1 = \varepsilon\left(-\lambda^2 \cos(\lambda x)\psi_{11} - \lambda\psi_{10} \sin(\lambda x)\right) \tag{52}$$

$$\theta_1 = \theta_{10} + \varepsilon\left(\cos(\lambda x)(t_{10}) - \lambda t_{11} \sin(\lambda x)\right) \tag{53}$$

Equations (51) to (53) are computed and are tabulated in Table 5. The above solutions agree very well with Rita and Alok [37]

2. Shifting the baffle to the left wall and comparing the solutions of stream-2 with Rita and Alok [37].

The boundary conditions for this case become

$$\theta_{20}=0,\ u_{20}=0,\ t_{20}=-\theta'_{10},\ \psi'_{20}=u'_{20},\ \psi_{20}=0,\quad \text{on } y=0$$
$$\theta_{20}=m,\ u_{20}=0,\ t_{20}=0,\ \psi'_{20}=0,\ \psi_{20}=0,\qquad \text{on } y=1 \tag{54}$$

$$t_{21}=0,\ \psi'_{21}=0,\ \psi_{21}=0,\ \text{on } y=0$$
$$t_{21}=0,\ \psi'_{21}=0,\ \psi_{21}=0,\qquad \text{on } y=1 \tag{55}$$

The solutions of stream-2 with above boundary conditions become

$$\theta_{20}=c_7y+c_8;\quad u_{20}=l_6y^3+l_7y^2+d_{11}y+d_{12} \tag{56}$$

$$t_{20}=c_9y+c_{10};\quad \psi_{20}=l_8y^4+\frac{d_{13}}{6}y^3+\frac{d_{14}}{2}y^2+d_{15}y+d_{16} \tag{57}$$

$$t_{21}=Pi\left(m_6y^6+m_7y^5+m_8y^4+m_9y^3+m_{10}y^2\right)+c_{11}y+c_{12},$$
$$\psi_{21}=i\left(\frac{n_{11}}{3024}y^9+\frac{n_{12}}{1680}y^8+\frac{n_{13}}{840}y^7+\frac{n_{14}}{360}y^6+\frac{n_{15}}{120}y^5+\frac{n_{16}}{24}y^4\right)+\frac{n_{17}}{24}y^4+\frac{d_{17}}{6}y^3+\frac{d_{18}}{2}y^2+d_{19}y+d_{20} \tag{58}$$

With the above solutions the velocity and temperature filed become

$$u_2=u_{20}+\varepsilon\left(-\cos(\lambda x)\psi'_{20}+\lambda\psi'_{21}\sin(\lambda x)\right) \tag{59}$$
$$v_2=\varepsilon\left(-\lambda^2\cos(\lambda x)\psi_{21}-\lambda\psi_{20}\sin(\lambda x)\right) \tag{60}$$
$$\theta_2=\theta_{20}+\varepsilon\left(\cos(\lambda x)(t_{20})-\lambda t_{21}\sin(\lambda x)\right) \tag{61}$$

Equations (59) to (61) are computed and are tabulated in Table 3b. These solutions agree very well with Rita and Alok [37]. All he constants appeared in the above equations are defined in the Appendix section

4. RESULTS AND DISCUSSION

Free convective flow and heat transfer of viscous fluid in a vertical channel one of whose walls is wavy, containing a thin conducting baffle is studied analytically. The non-linear partial differential equations governing the motion have been solved by a linearization technique wherein the flow is assumed to be of two parts; a mean part and a perturbed part. Exact solutions are obtained for the mean part and the perturbed pert is solved using long wave approximation. The Prandtl number, wave number, and amplitude are fixed as 0.7, 0.01, and 0.1, respectively for the computation, whereas the Grashof number, wall temperature ratio and product of non-dimensional wave number and space-coordinate are fixed as 20, -1, and 1.57079632, respectively for all the graphs except the varying one.

The effect of the Grashof number G on the main velocity is shown in figure 2a,b,c at three different baffle positions $\left(y^*=0.2,\ 0.5 \text{ and } 0.8\right)$. As the Grashof number increases, the main velocity u increases near the left (hot) wall and decreases at the right (cold) wall. The larger the value of G, the stronger the upward velocity. Especially, for sufficient large values of G, a flow reversal phenomenon is predicted near the right (cold) wall as shown in figure 2a, which can also be observed for Newtonian single passage flow examined by Aung and Warku [38]. For each graph the maximum point of the main velocity moves to the left (hotter) wall for increasing values of G and thus, the velocity decreases near the right (colder) wall. The effect of Grashof number G on the cross velocity is exactly opposite to the effect of G on the main velocity as seen in figure 3a,b,c. That is, as G increases, the cross velocity v decreases near the left (hot) wall and increases at the right (cold) wall. Also, as G increases, the maximum point of the cross velocity moves to the right (colder) wall and thus, the cross velocity decreases at the left (hot) wall. The effect of the Grashof number G on the temperature is shown in Table-1. It is noticed that the temperature remains almost invariant at all baffle positions for $G=5$ and $G=20$.

Figure 4a,b,c show the effect of the wall temperature ratio m on the main velocity ($m=-1$ means that the average of the temperatures of the two walls is equal to that of the static temperature, $m=0$ corresponds to the case that the temperature of the flat wall is equal to the static temperature, $m=1$ means that the wavy and flat wall are maintained at equal

temperature and $m > 1$ implies that the wall temperatures are unequal). As m increases, the main velocity u increases in both streams at the baffle positions 0.2, 0.5 and 0.8 and the flow reversal is observed in stream 2 for $m = -1$. It is also observed that the main velocity profile for $m = 0$ lies in between $m = -1$ (below) and 1 (above). When the baffle position is near the left wall, the variations of m are not very effective on the main velocity but its effect is dominant when the baffle position moves to the center and near to the right wall as seen in figure 4. The effect of m on the cross velocity is opposite to its effect on the main velocity. That is, as m increases the cross velocity decreases at all baffle positions as seen in figure 5a,b,c. The velocity profile for $m = 0$ lies in between $m = 1$ (below) and -1 (above). The effect of m on the cross velocity is not effective for the baffle position at the right wall when compared to the baffle position at the left and at the center of the channel. The effect of wall temperature ratio m on the temperature field is shown in figure 6a,b,c. As m increases, temperature increases at all the baffle positions and magnitude of promotion also remains the same for $y^* = 0.2,\ 0.5$ and 0.8.

The effect of the product of non-dimensional wave number and space coordinate, λx on the main velocity is shown in figure 7a,b,c. As λx increases, the main velocity increases near the wavy wall and reverses its direction near the baffle position and remains constant at the flat wall at all baffle positions. The effect of λx on the cross velocity is shown in figure 8a,b,c. As λx increases, the cross velocity decreases in stream 1 and increases in stream 2 for the baffle positions at the left and at the center of the walls. However, there is no effect of λx at the right wall when $y^* = 0.8$. The effect of λx on the temperature is presented in figure 9a,b,c. It is seen that increasing λx causes the temperature to decrease at the wavy wall while it remains unchanged at the flat wall for the baffle positions near the left, center and right walls. The magnitude of suppression remains the same at any position of the baffle.

The effect of the Grashof number is seen to increase the skin friction at both the wavy wall and at the flat wall at all baffle positions. The effect of wall temperature ratio m is to increase the skin friction at the wavy wall and decrease at the flat wall. The effects wave number and the amplitude parameter do not show much variation in the values of skin friction at both the walls as observed in Table-2a.

The effect of the Grashof number is found to increase the rate of heat transfer at the wavy wall and decrease at the flat wall in magnitude at all baffle positions. The effect of the wall temperature ratio is seen to decrease in magnitude, the heat transfer at both walls at all baffle positions. The effect of the wave number λ and amplitude parameter ε is found to increase in magnitude the rate of heat transfer at the wavy wall and decrease at the flat wall. However their effect on the rate of heat transfer is not very significant at both the walls as seen Table-2b.

The results obtained in 3.2 and the results obtained by Salah El Din [36] are displayed in Table-3a. This table shows that both the models show same values at all baffle positions which will justify the present model. The solutions obtained in section 3.3 and the solutions obtained by Rita and Alok [37] in the absence of viscoelastic parameter *K* are shown in Table-3b. When the baffle is shifted to the right wall (stream-1), the problem reduced to single passage whose solutions agree with Rita and Alok [37] which justifies the solutions of stream-1. To justify the solutions obtained in stream-2, the baffle is shifted to the right wall, which again reduces to single passage. The solutions obtained in stream-2 agree very well with Rita and Alok [37].

5. CONCLUSION

The flow and heat transfer of viscous fluid in a vertical wavy double-passage channel inserting a perfectly conducting baffle is investigated. According to the results, the following conclusions can be drawn:

1. The maxima of the main velocity profiles are obtained for increasing values of the Grashof number and the wall temperature ratio especially when the baffle position is in the middle of the channel. As λx increases, the main velocity decreases at the wavy wall and remains constant at the flat wall. The effects of the Grashof number, wall temperature ratio and λx on the cross velocity are exactly opposite to their effect on the main velocity.

2. The temperature profiles remain invariant with changes in the Grashof number. The effect of the wall temperature ratio promotes the temperature whereas λx reduces the temperature at the wavy wall while it remains constant at the flat wall. Again, these effects are more pronounced in the wider passage than in the narrower passage.

3. The skin friction increases at both the wavy and flat wall for increasing values of the Grashof number. The increase in the wall temperature ratio increases the skin friction at the wavy wall and decreases at the flat wall. Wave number and the amplitude parameter do not affect the skin friction at the wavy wall and at the flat wall significantly.

4. The effect of the Grashof number is found to increase the rate of heat transfer at the wavy wall and decrease at the flat wall in magnitude at all baffle positions. The effect of the wall temperature ratio is seen to decrease in magnitude, the heat transfer at both walls at all baffle positions. The effect of the wave number λ and amplitude parameter ε do not significantly affect the rate of heat transfer at both the walls.

5. The results of the present model agreed very well with the results obtained by Salah El Din [36] for both the walls to be flat. The results of the present model were also in good agreement with the results of Rita and Alok [37] for single passage with wavy wall.

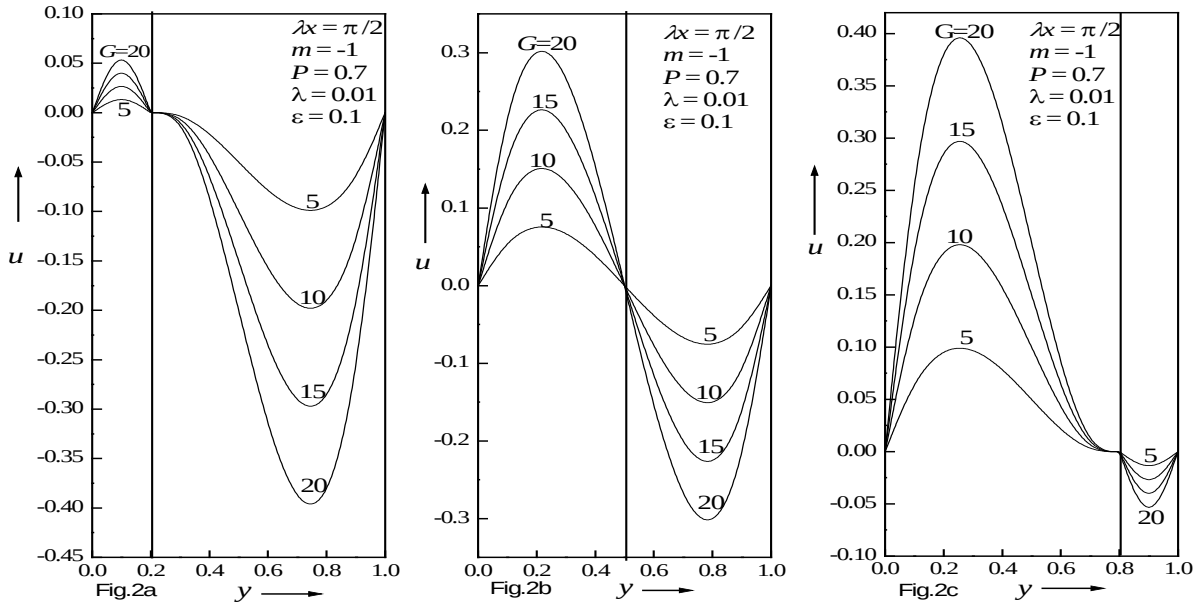

Fig. 2: Main velocity profiles for different values of Grashof number G.

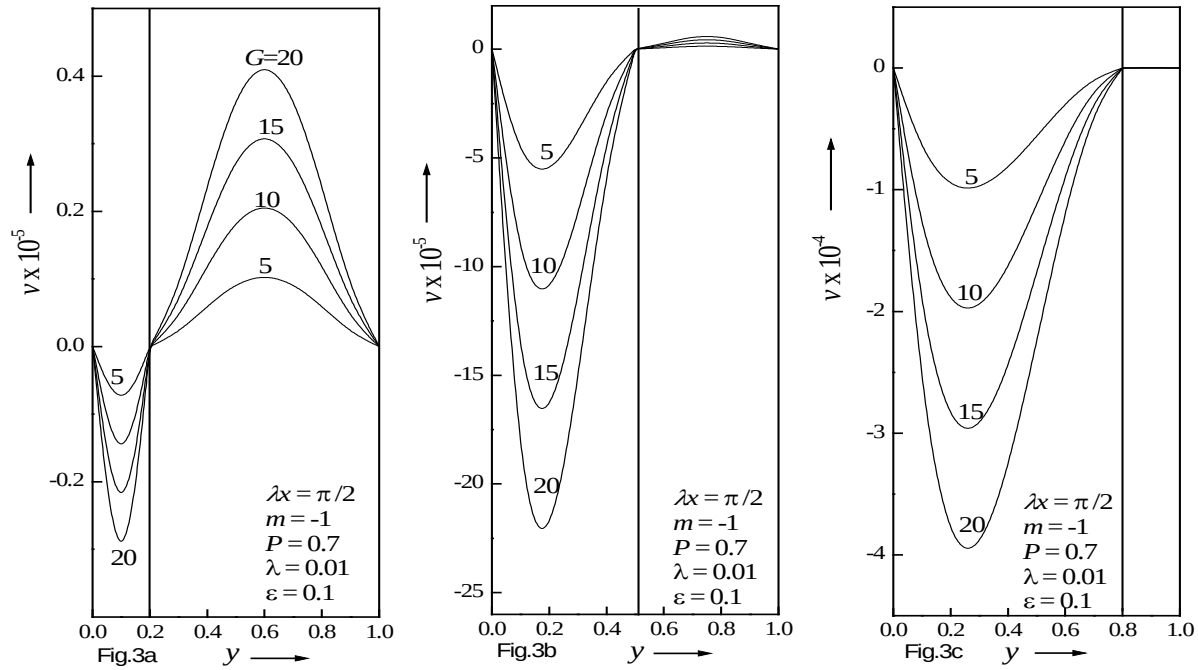

Fig. 3: Cross velocity profiles for different values of Grashof number G.

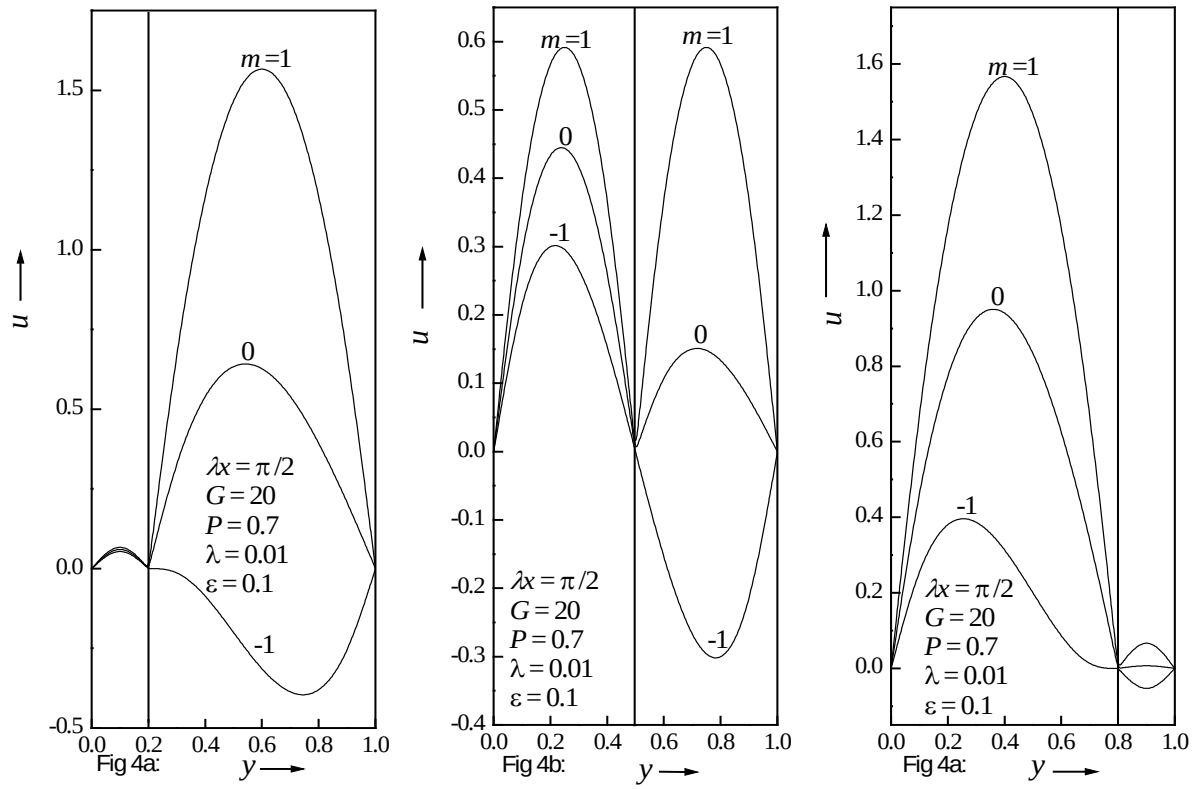

Fig. 4: Main velocity profiles for different values of wall temperature ratio m.

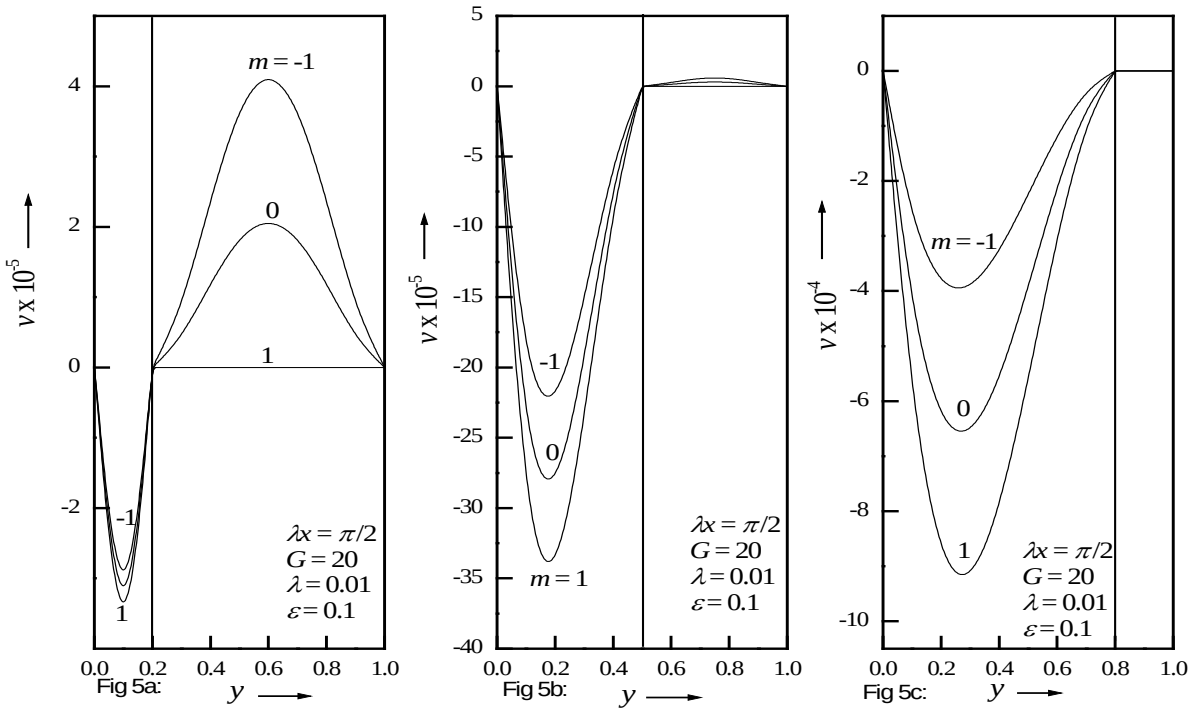

Fig. 5: Cross velocity profiles for different values of wall temperature ratio m.

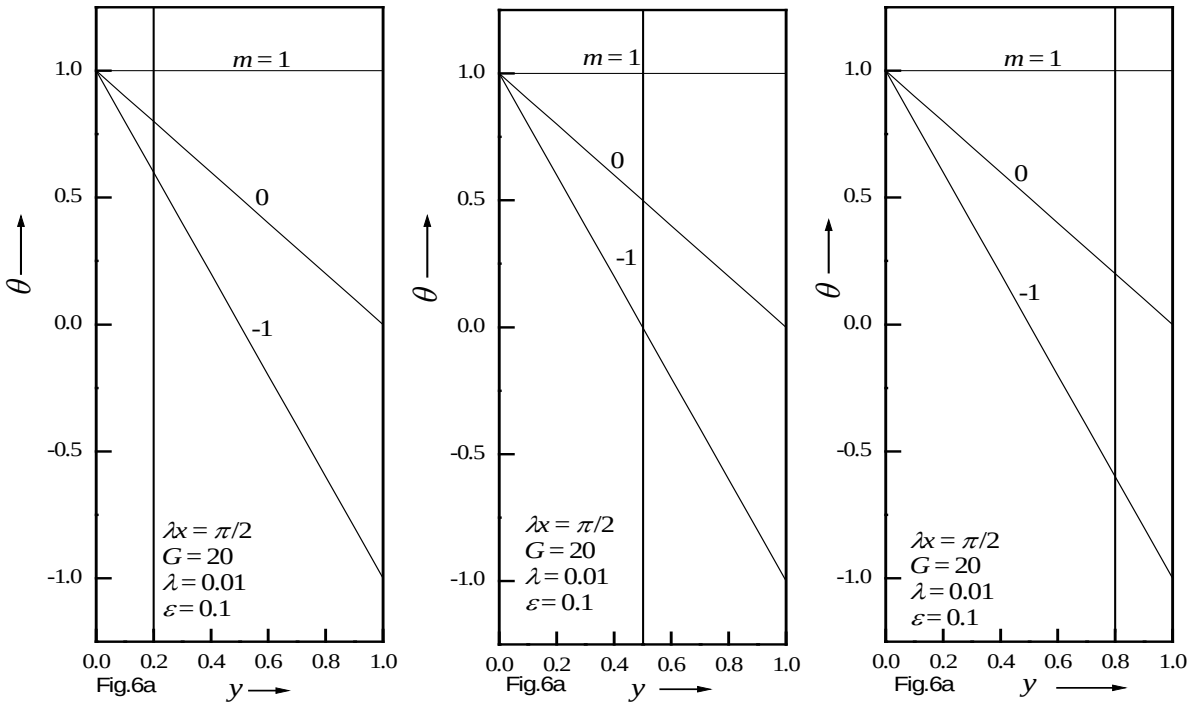

Fig. 6: Temperature profiles for different values of wall temperature ratio m.

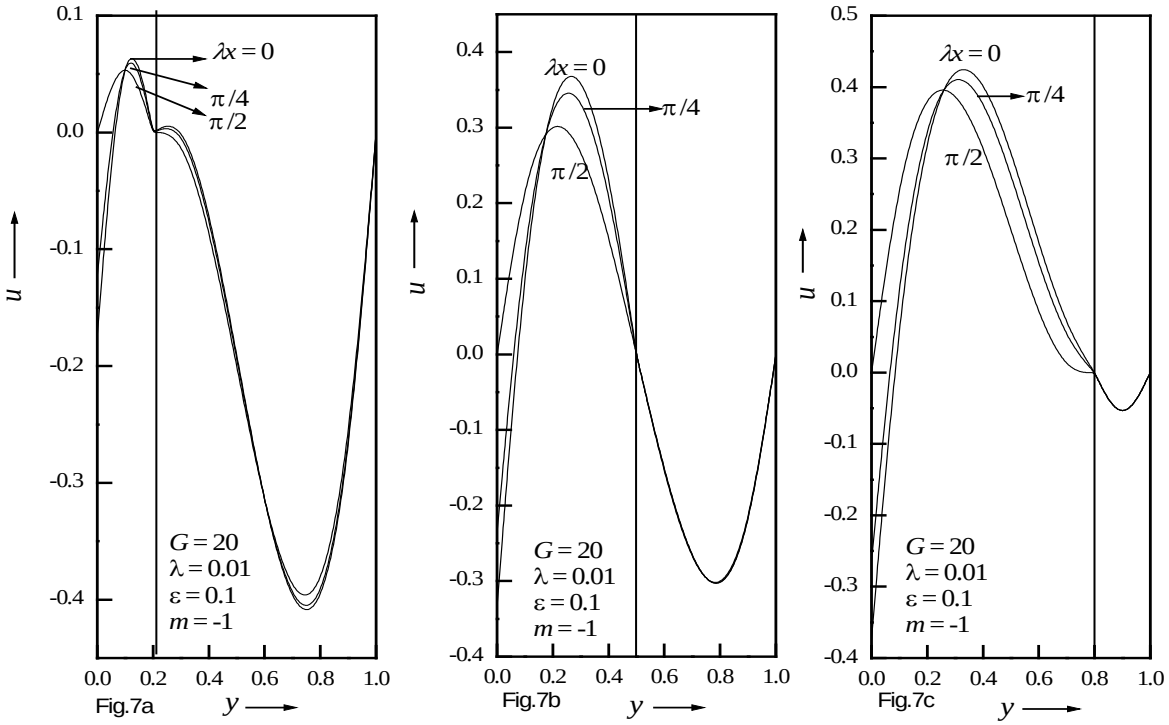

Fig. 7: Main velocity profiles for different values of λx.

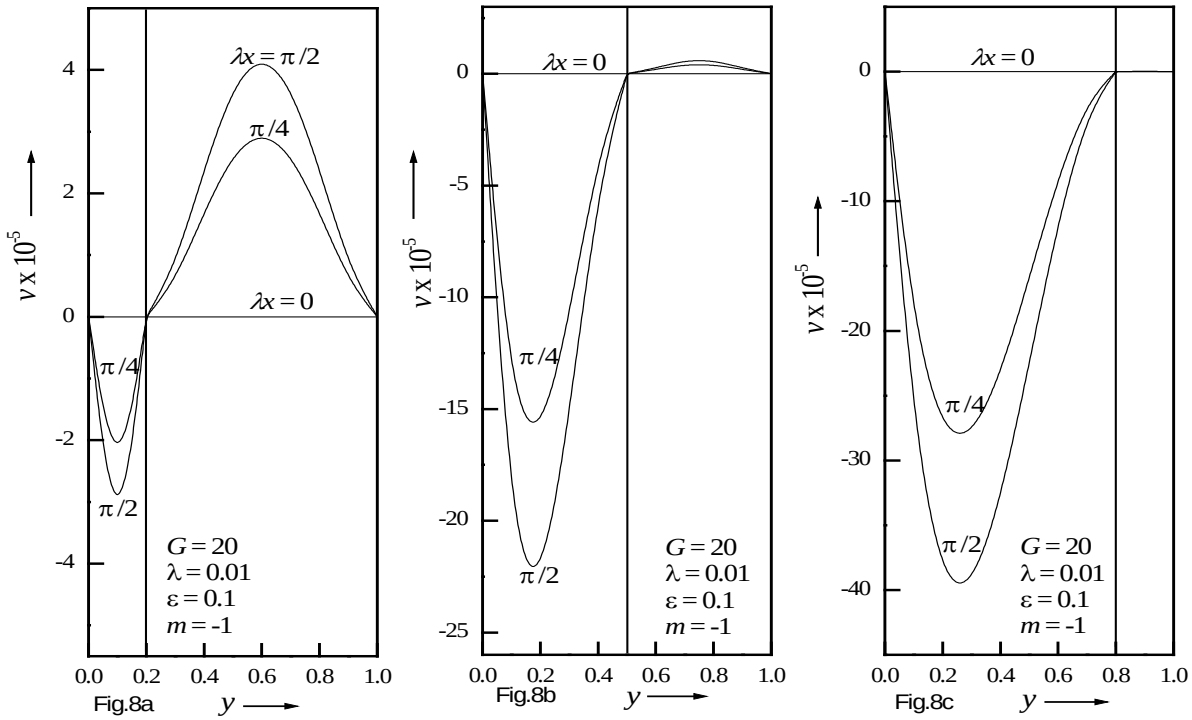

Fig. 8: Cross velocity profiles for different values of λx.

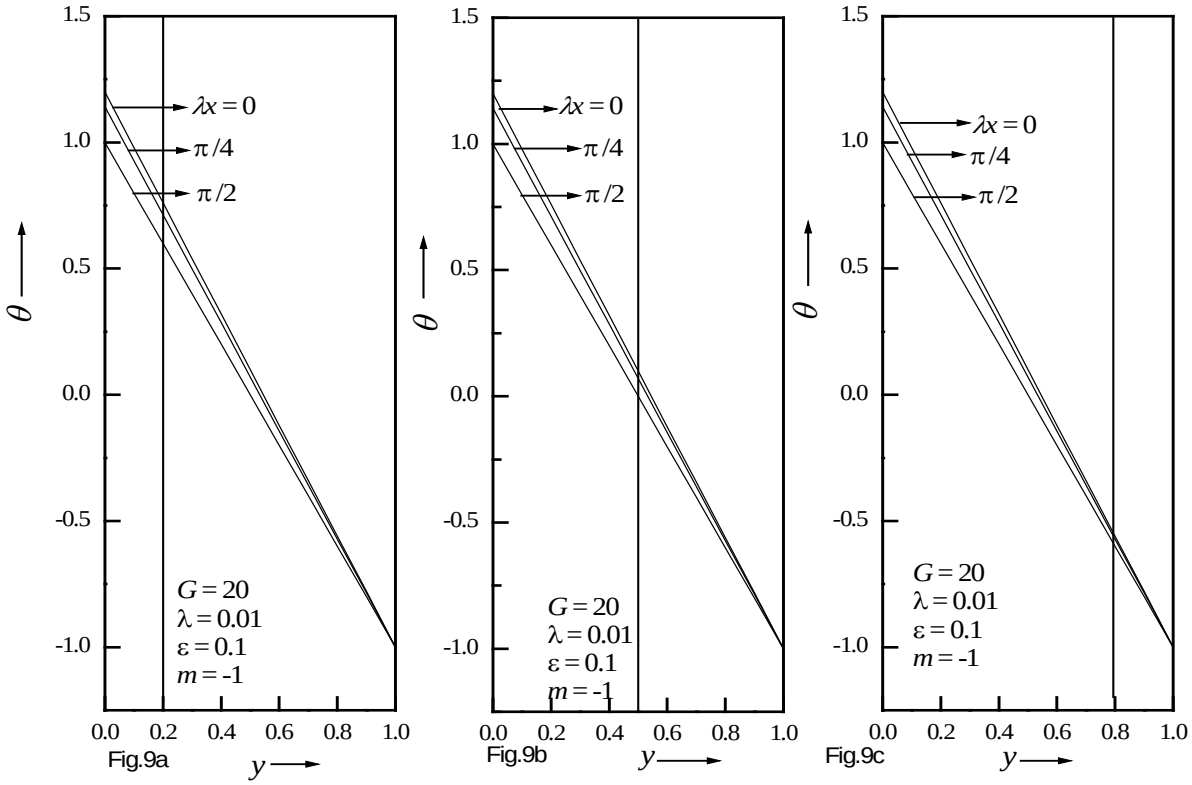

Fig. 9: Temperature profiles for different values of λx.

Table-1: Temperature values for different Grashof number and baffle positions with $m = 1,\ P = 0.7$ and $\lambda = 0.01$

y	$y^* = 0.2$		y	$y^* = 0.5$		y	$y^* = 0.8$	
	$G = 5$	$G = 20$		$G = 5$	$G = 20$		$G = 5$	$G = 20$
0	1.000000	1.000000	0	1.000000	1.000000	0	1.000000	1.000000
0.1	0.800000	0.799999	0.1	0.800000	0.800000	0.1	0.799999	0.799995
0.2	0.599999	0.599997	0.2	0.600000	0.600000	0.2	0.599998	0.599990
0.2	0.599999	0.599997	0.3	0.400000	0.400000	0.3	0.399997	0.399987
0.3	0.399999	0.399996	0.4	0.200000	0.199999	0.4	0.199996	0.199985
0.4	0.199999	0.199994	0.5	0	0	0.5	0	0
0.5	0	0	0.5	0	0	0.6	-0.200003	-0.200013
0.6	-0.200002	-0.200008	0.6	-0.200001	-0.200003	0.7	-0.400003	-0.400010
0.7	-0.400002	-0.400007	0.7	-0.400001	-0.400004	0.8	-0.600002	-0.600007
0.8	-0.600001	-0.600005	0.8	-0.600001	-0.600003	0.8	-0.600002	-0.600007
0.9	-0.800001	-0.800003	0.9	-0.800000	-0.800002	0.9	-0.800001	-0.800004
1.0	-1.000000	-1.000000	1	-1.000000	-1.000000	1	-1.000000	-1.000000

Table-2a: skin friction values at the wavy and flat wall.

	σ_w				σ_f		
G	$y^* = 0.2$	$y^* = 0.5$	$y^* = 0.8$	G	$y^* = 0.2$	$y^* = 0.5$	$y^* = 0.8$
20	1.73333	3.3333	3.73336	20	3.73332	3.33333	1.73333
100	8.66667	16.6665	18.6674	100	18.6664	16.6666	8.66661
200	17.334	33.3327	37.3361	200	37.3324	33.3327	17.3331
m				m			
-1	1.73333	3.3333	3.73336	-1	3.73332	3.33333	1.73333
0	1.86666	4.16664	5.8666	0	-2.1333	-0.83332	-0.13333
1	2.0000	4.99997	7.9998	1	-8	-5	-2
λ				λ			
0	1.73333	3.3333	3.73333	0	3.73333	3.3333	1.73333
0.1	1.73334	3.33327	3.73361	0.1	3.73324	3.3333	1.73331
0.5	1.73335	3.33303	3.73472	0.5	3.73288	3.33315	1.73322
ε				ε			
0	1.73333	3.33333	3.73333	0	3.73333	3.3333	1.73333
0.1	1.73333	3.3333	3.73336	0.1	3.73332	3.33333	1.73333
0.5	1.73333	3.3333	3.73347	0.5	3.73329	3.33331	1.73332

Table-2b: Nusselt number values at the wavy and flat wall.

	Nu_w				Nu_f		
G	$y^* = 0.2$	$y^* = 0.5$	$y^* = 0.8$	G	$y^* = 0.2$	$y^* = 0.5$	$y^* = 0.8$
20	-2.00001	-2	-2.00005	20	-1.99997	-1.99998	-1.99996
100	-2.00005	-1.99999	-2.00025	100	-1.99986	-1.99991	-1.99982
200	-2.00011	-1.99998	-2.0005	200	-1.99971	-1.99983	-1.99964
m				m			
-1	-2.00001	-2	-2.00005	-1	-1.99997	-1.99998	-1.99996
0	-0.99994	-0.99998	-0.99999	0	-1.00006	-1.00001	-1.00001
1	0	0	0	1	0	0	0
λ				λ			
0	-2	-2	-2	0	-2	-2	-2
0.1	-2.00011	-1.99998	-2.0005	0.1	-1.99971	-1.99983	-1.99964

0.5	-2.00053	-1.99988	-2.00251	0.5	-1.99857	-1.99915	-1.99822
ε				ε			
0	-2	-2	-2	0	-2	-2	-2
0.1	-2.00001	-2	-2.00005	0.1	-1.99997	-1.99998	-1.99996
0.5	-2.00005	-1.99999	-2.00025	0.5	-1.99986	-1.99991	-1.99982

Table-3a: Comparison of velocity at different baffle positions with Salah El Din [36] for $G = 20,\ m = 1,\ P = 0.7,$ and $\lambda = 0.01$

y	Present Model	Salah El Din [36]	y	Present Model	Salah El Din [36]	y	Present Model	Salah El Din [36]
	$y^* = 0.2$	$y^* = 0.2$		$y^* = 0.5$	$y^* = 0.5$		$y^* = 0.8$	$y^* = 0.8$
0	0	0	0	0	0	0	0	0
0.1	-0.04	-0.04	0.1	-0.12	-0.12	0.1	-0.14	-0.14
0.2	0	0	0.2	-0.16	-0.16	0.2	-0.2	-0.2
0.2	0	0	0.3	-0.14	-0.14	0.3	-0.2	-0.2
0.3	0	0	0.4	-0.08	-0.08	0.4	-0.16	-0.16
0.4	0.04	0.04	0.5	0	0	0.5	-0.1	-0.1
0.5	0.1	0.1	0.5	0	0	0.6	-0.04	-0.04
0.6	0.16	0.16	0.6	0.08	0.08	0.7	0	0
0.7	0.2	0.2	0.7	0.14	0.14	0.8	0	0
0.8	0.2	0.2	0.8	0.16	0.16	0.8	0.04	0.04
0.9	0.14	0.14	0.9	0.12	0.12	0.9	0	0
1	0	0	1	0	0	1	0	0

Table-3b: Validity of the present model with stream-1 (shifting the baffle to the right wall) and stream-2 (shifting the baffle to the left wall) with Rita and Alok [37] for $G = 20,\ m = 1,\ P = 0.7$ and $\lambda = 0.01$.

y	Present Model						Rita and Alok [37] for viscoelastic parameter $K = 0$		
	Stream-1			Stream-2					
	u_1	v_1	θ_1	u_2	v_2	θ_2	u	v	θ
0.0	0	0	1.0	0	0	1.0	0	0	1.0
0.1	0.90	-8.1E-4	1.0	0.90	-8.1E-4	1.0	0.90	-8.1E-4	1.0
0.2	1.60	-0.00128	1.0	1.60	-0.00128	1.0	1.60	-0.00128	1.0
0.3	2.10	-0.00147	1.0	2.10	-0.00147	1.0	2.10	-0.00147	1.0
0.4	2.40	-0.00144	1.0	2.40	-0.00144	1.0	2.40	-0.00144	1.0
0.5	2.50	-0.00125	1.0	2.50	-0.00125	1.0	2.50	-0.00125	1.0
0.6	2.40	-9.6E-4	1.0	2.40	-9.6E-4	1.0	2.40	-9.6E-4	1.0
0.7	2.10	-6.3E-4	1.0	2.10	-6.3E-4	1.0	2.10	-6.3E-4	1.0
0.8	1.60	-3.2E-4	1.0	1.60	-3.2E-4	1.0	1.60	-3.2E-4	1.0
0.9	0.90	-9E-5	1.0	0.90	-9E-5	1.0	0.90	-9E-5	1.0
1.0	0	0	1.0	0	0	1.0	0	0	1.0

NOMENCLATURE

d	channel width
d^*	width of passage 1
c_p	dimensionless specific heat at constant pressure
g_x	acceleration due to gravity
G	Grashof number $\left(d^3 g_x \beta (T_w - T_s)/\nu^2\right)$
k	wavelength
Nu	Nusselt number
$\bar{p}$	pressure
p	dimensionless pressure
P	Prandtl number $\left(c_p \eta_0 / k\right)$
p_s	static pressure

rp	real part
i p	imaginary part
T	temperature
T_s	static temperature
U,V	velocities along X and Y directions
u,v	dimensionless velocities
X,Y	space co-ordinates
x,y	dimensionless space co-ordinates

GREEK SYMBOLS

β	dimensionless co-efficient of thermal expansion
ε	non-dimensional amplitude parameter $\left(\varepsilon^*/d\right)$
ε^*	amplitude
λ	non-dimensional wave number $\left(k/d\right)$
μ	viscosity
ν	kinematic viscosity
θ	dimensionless temperature
ρ	density
ρ_0	static density
σ_{xy}	skin friction
ψ	stream function

SUBSCRIPTS

i refer quantities for the fluids in stream 1 and stream 2, respectively.

Appendix

$\theta_{10} = c_1 y + c_2$; $u_{10} = l_1 y^3 + l_2 y^2 + d_1 y + d_2$; $\theta_{20} = c_7 y + c_8$; $u_{20} = l_6 y^3 + l_7 y^2 + d_{11} y + d_{12}$;

$$u_{11} = -\cos(\lambda x)\left(4l_3 y^4 + \frac{d_3}{2} y^2 + d_4 y + d_5\right) + \lambda \sin(\lambda x)\left(\frac{n_1}{336} y^8 + \frac{n_2}{210} y^7 + \frac{n_3}{120} y^6 + \frac{n_4}{60} y^5 + \frac{n_5}{24} y^4 + \frac{n_6}{6} y^3 + \frac{n_7}{6} y^3 + \frac{d_7}{2} y^2 + d_8 y + d_9\right)$$

$$u_{21} = -\cos(\lambda x)\left(4l_8 y^3 + \frac{d_{13}}{2} y^2 + d_{14} y + d_{15}\right) + \lambda \sin(\lambda x)\left(\frac{n_{11}}{336} y^8 + \frac{n_{12}}{210} y^7 + \frac{n_{13}}{120} y^6 + \frac{n_{14}}{60} y^5 + \frac{n_{15}}{24} y^4 + \frac{n_{16}}{6} y^3 + \frac{n_{17}}{6} y^3 + \frac{d_{17}}{2} y^2 + d_{18} y + d_{19}\right)$$

$$v_{11} = -\lambda \sin(\lambda x)\left(l_3 y^4 + \frac{d_3}{6} y^3 + \frac{d_4}{2} y^2 + d_5 y + d_6\right) - \lambda^2 \cos(\lambda x)\left(\frac{n_1}{3024} y^9 + \frac{n_2}{1680} y^8 + \frac{n_3}{840} y^7 + \frac{n_4}{360} y^7 + \frac{n_5}{120} y^6 + \frac{n_6}{24} y^5 + \frac{n_7}{24} y^4 + \frac{d_7}{6} y^3 + \frac{d_8}{2} y^2 + d_9 y + d_{10}\right)$$

$$v_{21} = -\lambda \sin(\lambda x)(l_8 y^4 + \frac{d_{13}}{6} y^3 + \frac{d_{14}}{2} y^2 + d_{15} y + d_{16}) - \lambda^2 \cos(\lambda x)\left(\frac{n_{11}}{3024} y^9 + \frac{n_{12}}{1680} y^8 + \frac{n_{13}}{840} y^7 + \frac{n_{14}}{360} y^6 + \frac{n_{15}}{120} y^5 + \frac{n_{16}}{24} y^4 + \frac{n_{17}}{24} y^4 + \frac{d_{17}}{6} y^3 + \frac{d_{18}}{2} y^2 + d_{19} y + d_{20}\right)$$

$$\theta_1 = \cos(\lambda x)(c_3 y + c_4) - \lambda \sin(\lambda x)(P(m_1 y^6 + m_2 y^5 + m_3 y^4 + m_4 y^3 + m_5 y^2) + c_5 y + c_6)$$

$$\theta_{21} = \cos(\lambda x)(c_9 y + c_{10}) - \lambda \sin(\lambda x)\left(P\left(m_6 y^6 + m_7 y^5 + m_8 y^4 + m_9 y^3 + m_{10} y^2\right) + c_{11} y + c_{12}\right)$$

$$u_1 = l_1 y^3 + l_2 y^2 + d_1 y + d_2 + \varepsilon\left(-\cos(\lambda x)\left(4l_3 y^3 + \frac{d_3}{2} y^2 + d_4 y + d_5\right) + \lambda \sin(\lambda x)\left(\frac{n_1}{336} y^8 + \frac{n_2}{210} y^7 + \frac{n_3}{120} y^6 + \frac{n_4}{60} y^5 + \frac{n_5}{24} y^4 + \frac{n_6}{6} y^3 + \frac{n_7}{6} y^3 + \frac{d_7}{2} y^2 + d_8 y + d_9\right)\right)$$

$$u_2 = l_7 y^4 + l_8 y^3 + l_9 y^2 + d_{11} y + d_{12} + \varepsilon\left(-\cos(\lambda x)\left(4l_8 y^3 + \frac{d_{13}}{2} y^2 + d_{14} y + d_{15}\right) + \lambda \sin(\lambda x)\left(\frac{n_{11}}{336} y^8 + \frac{n_{12}}{210} y^7 + \frac{n_{13}}{120} y^6 + \frac{n_{14}}{60} y^5 + \frac{n_{15}}{24} y^4 + \frac{n_{16}}{6} y^3 + \frac{n_{17}}{6} y^3 + \frac{d_{17}}{2} y^2 + d_{18} y + d_{19}\right)\right)$$

$$v_1 = \varepsilon\left(-\lambda \sin(\lambda x)\left(l_3 y^4 + \frac{d_3}{6} y^3 + \frac{d_4}{2} y^2 + d_5 y + d_6\right) - \lambda^2 \cos(\lambda x)\left(\frac{n_1}{3024} y^9 + \frac{n_2}{1680} y^8 + \frac{n_3}{840} y^7 + \frac{n_4}{360} y^7 + \frac{n_5}{120} y^6 + \frac{n_6}{24} y^5 + \frac{n_7}{24} y^4 + \frac{d_7}{6} y^3 + \frac{d_8}{2} y^2 + d_9 y + d_{10}\right)\right)$$

$$v_2 = \varepsilon\left(-\lambda \sin(\lambda x)(l_8 y^4 + \frac{d_{13}}{6} y^3 + \frac{d_{14}}{2} y^2 + d_{15} y + d_{16}) - \lambda^2 \cos(\lambda x)\left(\frac{n_{11}}{3024} y^9 + \frac{n_{12}}{1680} y^8 + \frac{n_{13}}{840} y^7 + \frac{n_{14}}{360} y^6 + \frac{n_{15}}{120} y^5 + \frac{n_{16}}{24} y^4 + \frac{n_{17}}{24} y^4 + \frac{d_{17}}{6} y^3 + \frac{d_{18}}{2} y^2 + d_{19} y + d_{20} \right)\right)$$

$$\theta_1 = c_1 y + c_2 + \varepsilon\left(\cos(\lambda x)(c_3 y + c_4) - \lambda \sin(\lambda x)(P(m_1 y^6 + m_2 y^5 + m_3 y^4 + m_4 y^3 + m_5 y^2) + c_5 y + c_6)\right)$$

$$\theta_2 = c_7 y + c_8 + \varepsilon\left(\cos(\lambda x)(c_9 y + c_{10}) - \lambda \sin(\lambda x)\left(P\left(m_6 y^6 + m_7 y^5 + m_8 y^4 + m_9 y^3 + m_{10} y^2\right) + c_{11} y + c_{12}\right)\right)$$

$c_1 = m-1,\ c_2 = 1,\ c_3 = m-1,\ c_4 = -(m-1),\ c_9 = m-1,\ c_{10} = -(m-1),\ c_7 = m-1,\ c_8 = 1,\ d_2 = 0,\ d_6 = 0,\ d_9 = 0,$

$d_{10} = 0,\ l_1 = \frac{-Gc_1}{6},\ l_2 = \frac{-Gc_2}{2},\ l_3 = \frac{Gc_3}{24},\ d_1 = -(l_1 y^{*2} + l_2 y^*),\ d_5 = -(l_1 y^{*2} + l_2 y^*),\ d_3 = -12 l_3 y^* + \frac{6d_5}{y^{*2}},$

$$d_4 = \frac{1}{y^*}\left(-d_5 - 4l_3 y^{*3} - \frac{d_3 y^{*2}}{2} \right),\ l_4 = \frac{d_3}{6},\ l_5 = \frac{d_4}{2},\ l_6 = \frac{-Gc_7}{6},\ l_7 = \frac{-Gc_8}{2},\ d_{11} = \frac{l_6(1-y^{*3}) + l_7(1-y^{*2})}{y^* - 1},$$

$$d_{12} = -l_6 - l_7 - d_{11},\ l_8 = \frac{Gc_9}{24},\ d_{13} = \frac{-l_8((1-y^{*4}) - 4(1-y^*) + 2(1-y^{*3})(1-y^*))}{\frac{(1-y^{*3})}{6} + \frac{(1-y^{*2})(1-y^*)}{4} - \frac{(1-y^*)}{2}},\ d_{14} = \frac{-4l_8\left(1-y^{*3}\right) - \frac{d_{13}}{2}\left(1-y^{*2}\right)}{\left(1-y^*\right)},$$

$$d_{15} = -4l_8 y^{*3} - \frac{d_{13}}{2} y^{*2} - d_{14} y^*,\ d_{16} = -l_8 - \frac{d_{13}}{6} - \frac{d_{14}}{2} - d_{15},\ l_9 = \frac{d_{13}}{6},\ l_{10} = \frac{d_{14}}{2},\ m_1 = \frac{c_3 l_1 + c_1 l_3}{30},\ m_2 = \frac{c_3 l_2 + c_4 l_1 + c_1 l_4}{20},$$

$$m_3 = \frac{c_3 d_1 + c_4 l_2 + c_1 l_5}{12},\ m_4 = \frac{c_3 d_2 + c_4 d_1 + c_1 d_5}{6},\ m_5 = \frac{c_4 d_2}{2},\ m_6 = \frac{c_9 l_6 + c_7 l_8}{30},\ m_7 = \frac{c_9 l_7 + c_1 l_6 + c_7 l_9}{20},$$

$$m_8 = \frac{c_9 d_{11} + c_{10} l_7 + c_7 l_{10}}{12},\ m_9 = \frac{c_9 d_{12} + c_{10} d_{11} + c_7 d_{15}}{6},\ m_{10} = \frac{c_{10} d_{12} + c_7 d_{16}}{2},$$

$$c_{12} = iP\left(\left(5m_6 y^{*6} + 4m_7 y^{*5} + 3m_8 y^{*4} + 2m_9 y^{*3} + m_{10} y^{*2}\right) - \left(5m_1 y^{*6} + 4m_2 y^{*5} + 3m_3 y^{*4} + 2m_4 y^{*3} + m_5 y^{*2}\right)\right),$$

$$c_{11} = -Pi\left(m_6 + m_7 + m_8 + m_9 + m_{10}\right) - c_{12},$$

$$c_5 = iP\left(6m_6 y^{*5} + 5m_7 y^{*4} + 4m_8 y^{*3} + 3m_9 y^{*2} + 2m_1\ y^*\right) - iP_0\left(6m_1 y^{*5} + 5m_2 y^{*4} + 4m_3 y^{*3} + 3m_4 y^{*2} + 2m_5 y^*\right) + c_1\ ,$$

$$n_1 = 6l_1 l_3 + 6GPm_1,\ n_2 = 10l_3 l_2 + 5GPm_2,\ n_3 = 12d_1 l_3 + 4l_4 l_2 - 4l_1 l_5 + 4GPm_3,$$

$$n_4 = 12l_3 d_2 + 6l_4 d_1 - 6l_1 d_5 + 3GPm_4,\ n_5 = 6l_4 d_2 + 2l_5 d_1 - 6l_1 d_6 - 2l_2 d_5 + 2GPm_5,\ n_6 = 2l_5 d_2 - 2l_2 d_6,\ n_7 = GC_5,$$

$$d_7 = -\frac{n_1 y^{*6}}{72} - \frac{3n_2 y^{*5}}{140} - \frac{n_3 y^{*4}}{28} - \frac{n_4 y^{*3}}{15} - \frac{3n_5 y^{*2}}{20} - \frac{n_6 y^*}{2} - \frac{n_7 y^*}{2},$$

$$d_8 = -\frac{n_1 y^{*7}}{1512} - \frac{n_2 y^{*6}}{840} - \frac{n_3 y^{*5}}{420} - \frac{n_4 y^{*4}}{180} - \frac{n_5 y^{*3}}{60} - \frac{n_6 y^{*2}}{12} - \frac{n_7 y^{*2}}{12} - \frac{d_7 y^*}{3},\ n_{11} = 6l_6 l_8 + 6GPm_6,\ n_{12} = 10l_7 l_8 + 5GPm_7,$$

$$n_{13} = 12d_{11} l_8 + 4l_9 l_7 - 4l_6 l_{10} + 4GPm_8,\ n_{14} = 12l_8 d_{12} + 6l_9 d_{11} - 6l_6 d_{15} + 3GPm_9,$$

$$n_{15} = 6l_9 d_{12} + 2l_{10} d_{11} - 6l_6 d_{16} - 2l_7 d_{15} + 2GPm_{10},\ n_{16} = 2l_{10} d_{12} - 2l_7 d_{16},\ n_{17} = GC_{11},$$

$$Z_1 = \frac{n_{11}\left(1-y^{*8}\right)}{336} + \frac{n_{12}\left(1-y^{*7}\right)}{210} + \frac{n_{13}\left(1-y^{*6}\right)}{120} + \frac{n_{14}\left(1-y^{*5}\right)}{60} + \frac{n_{15}\left(1-y^{*4}\right)}{24} + \frac{n_{16}\left(1-y^{*3}\right)}{6} + \frac{n_{17}\left(1-y^{*3}\right)}{6},$$

$$Z_2 = \frac{n_{11}\left(1-y^{*9}\right)}{3024} - \frac{n_{11}\left(1-y^*\right)}{336} + \frac{n_{12}\left(1-y^{*8}\right)}{1680} - \frac{n_{12}\left(1-y^*\right)}{210} + \frac{n_{13}\left(1-y^{*7}\right)}{840} - \frac{n_{13}\left(1-y^*\right)}{120} + \frac{n_{14}\left(1-y^{*6}\right)}{360} - \frac{n_{14}\left(1-y^*\right)}{60} + \frac{n_{15}\left(1-y^{*5}\right)}{120} - \frac{n_{15}\left(1-y^*\right)}{24},$$

$$+ \frac{n_{16}\left(1-y^{*4}\right)}{24} - \frac{n_{16}\left(1-y^*\right)}{6} + \frac{n_{17}\left(1-y^{*4}\right)}{24} - \frac{n_{17}\left(1-y^*\right)}{6}$$

$$d_{17}=-Z_2-Z_1\frac{\left(1-y^*\right)}{2}\Bigg/\left(\frac{1-y^{*^3}}{6}+\frac{\left(1-y^{*^2}\right)\left(1-y^*\right)}{4}-\frac{\left(1-y^*\right)}{2}\right),\ d_{18}=-Z_1-\frac{d_{17}\left(1-y^{*2}\right)}{2\left(1-y^*\right)},$$

$$d_{19}=-\frac{n_{11}}{336}-\frac{n_{12}}{210}-\frac{n_{13}}{120}-\frac{n_{15}}{60}-\frac{n_{16}}{24}-\frac{n_{17}}{6}-\frac{n_{18}}{6}-\frac{d_{17}}{2}-d_{18},$$

$$d_{20}=-\frac{n_{11}y^{*^9}}{5040}-\frac{n_{12}y^{*^8}}{3024}-\frac{n_{13}y^{*^7}}{1680}-\frac{n_{14}y^{*^6}}{840}-\frac{n_{15}y^{*^5}}{360}-\frac{n_{16}y^{*^4}}{120}-\frac{n_{17}y^{*^4}}{24}-\frac{d_{17}y^{*^3}}{6}-\frac{d_{18}y^{*^2}}{2}-d_{19}y^*.$$

Case 3.2 Comparison of the Solutions with Salah El Din [36] in the presence of baffle

$$\theta_{10}=y-\frac{1}{2},\ \theta_{20}=y-\frac{1}{2}$$

$$u_{10}=-\frac{G}{2}\left(\frac{y^3}{3}-\frac{y^2}{2}\right)+d_1y+d_2,\ u_{20}=-\frac{G}{2}\left(\frac{y^3}{3}-\frac{y^2}{2}\right)+d_3y+d_4$$

$$d_1=-\frac{G}{2}\left(\frac{y^{*2}}{3}-\frac{y^*}{2}\right),\ d_2=0,\ d_3=-c_8-\frac{G}{12},\ d_4=\frac{G}{2\left(1-y^*\right)}\left(\frac{y^{*3}}{3}-\frac{y^{*2}}{2}+\frac{y^*}{6}\right)$$

Case 3.3 Comparison of the Solutions with Rita and Alok [37] in the absence of baffle

1. Shifting the baffle to the left wall and comparing the solutions of stream-1 with Rita and Alok [37].

$$c_1=m-1,\ c_2=1,\ l_1=\frac{-Gc_1}{6},\ l_2=\frac{-Gc_2}{2},\ d_1=-l_1-l_2,\ d_2=0,\ c_3=m-1,\ c_4=-\left(m-1\right),\ l_3=\frac{Gc_3}{24},\ d_3=-12l_3+6d_5,$$

$$d_4=-d_5-4l_3-\frac{d_3}{2},\ d_5=-l_1-l_2,\ d_6=0,\ m_1=\frac{c_3l_1+c_1l_3}{30},\ m_2=\frac{c_3l_2+c_4l_1+c_1l_4}{20},\ m_3=\frac{c_3d_1+c_4l_2+c_1l_5}{12},$$

$$m_4=\frac{c_3d_2+c_4d_1+c_1d_5}{6},\ m_5=\frac{c_4d_2}{2},\ c_5=iP\left(6m_6+5m_7+4m_8+3m_9+2m_1\ \right)-iP_0\left(6m_1+5m_2+4m_3+3m_4+2m_5\right)+c_1\ ,$$

$$c_6=0,\ n_1=6l_1l_3+6GPm_1,\ n_2=10l_3l_2+5GPm_2,\ n_3=12d_1l_3+4l_4l_2-4l_1l_5+4GPm_3,$$

$$n_4=12l_3d_2+6l_4d_1-6l_1d_5+3GPm_4,\ n_5=6l_4d_2+2l_5d_1-6l_1d_6-2l_2d_5+2GPm_5,\ n_6=2l_5d_2-2l_2d_6,\ n_7=GC_5,$$

$$d_7=-\frac{n_1}{72}-\frac{3n_2}{140}-\frac{n_3}{28}-\frac{n_4}{15}-\frac{3n_5}{20}-\frac{n_6}{2}-\frac{n_7}{2},\ d_8=-\frac{n_1}{1512}-\frac{n_2}{840}-\frac{n_3}{420}-\frac{n_4}{180}-\frac{n_5}{60}-\frac{n_6}{12}-\frac{n_7}{12}-\frac{d_7}{3},\ d_9=0,\ d_{10}=0.$$

2. Shifting the baffle to the right wall and comparing the solutions of stream-1 with Rita and Alok [37].

$$c_9=m-1,\ c_{10}=-\left(m-1\right),\ c_7=m-1,\ c_8=1,\ l_4=\frac{d_3}{6},\ l_5=\frac{d_4}{2},\ l_6=\frac{-Gc_7}{6},\ l_7=\frac{-Gc_8}{2},\ d_{11}=-l_6-l_7,$$

$$d_{12}=-l_6-l_7-d_{11},\ l_8=\frac{Gc_9}{24},\ d_{13}=6l_8,\ d_{14}=-4l_8-\frac{d_{13}}{2},\ d_{15}=-4l_8-\frac{d_{13}}{2}-d_{14},\ d_{16}=-l_8-\frac{d_{13}}{6}-\frac{d_{14}}{2}-d_{15},\ l_9=\frac{d_{13}}{6},$$

$$l_{10}=\frac{d_{14}}{2},\ m_6=\frac{c_9l_6+c_7l_8}{30},\ m_7=\frac{c_9l_7+c_1\ l_6+c_7l_9}{20},\ m_8=\frac{c_9d_{11}+c_{10}l_7+c_7l_{10}}{12},\ m_9=\frac{c_9d_{12}+c_{10}d_{11}+c_7d_{15}}{6},$$

$$m_{10}=\frac{c_{10}d_{12}+c_7d_{16}}{2},\ c_{12}=iP\left(\left(5m_6+4m_7+3m_8+2m_9+m_{10}\right)-\left(5m_1+4m_2+3m_3+2m_4+m_5\right)\right),$$

$$c_{11}=-Pi\left(m_6+m_7+m_8+m_9+m_{10}\right)-c_{12},$$

$$n_{11}=6l_6l_8+6GPm_6,\ n_{12}=10l_7l_8+5GPm_7,\ n_{13}=12d_{11}l_8+4l_9l_7-4l_6l_{10}+4GPm_8,\ n_{14}=12l_8d_{12}+6l_9d_{11}-6l_6d_{15}+3GPm_9,$$

$$n_{15}=6l_9d_{12}+2l_{10}d_{11}-6l_6d_{16}-2l_7d_{15}+2GPm_{10},\ n_{16}=2l_{10}d_{12}-2l_7d_{16},\ n_{17}=GC_{11},$$

$$Z_1=\frac{n_{11}}{336}+\frac{n_{12}}{210}+\frac{n_{13}}{120}+\frac{n_{14}}{60}+\frac{n_{15}}{24}+\frac{n_{16}}{6}+\frac{n_{17}}{6},Z_2=-\frac{8n_{11}}{3024}-\frac{7n_{12}}{1680}-\frac{6n_{13}}{840}-\frac{5n_{14}}{360}-\frac{4n_{15}}{120}-\frac{3n_{16}}{24}-\frac{2n_{17}}{24},$$

$$d_{17}=-Z_2+\frac{Z_1}{24},\ d_{18}=-Z_1-\frac{d_{17}}{2},\ d_{19}=-\frac{n_{11}}{336}-\frac{n_{12}}{210}-\frac{n_{13}}{120}-\frac{n_{15}}{60}-\frac{n_{16}}{24}-\frac{n_{17}}{6}-\frac{n_{18}}{6}-\frac{d_{17}}{2}-d_{18},$$

$$d_{20}=-\frac{n_{11}}{5040}-\frac{n_{12}}{3024}-\frac{n_{13}}{1680}-\frac{n_{14}}{840}-\frac{n_{15}}{360}-\frac{n_{16}}{120}-\frac{n_{17}}{24}-\frac{d_{17}}{6}-\frac{d_{18}}{2}-d_{19}.$$

6. REFERENCES

[1] Ostrach, S., An analysis of laminar free-convection flow and heat transfer about a flat plat parallel to the direction of the generating body force, NACA, TN-2635, Accession number-93R12788, 1952.

[2] Jaloria., Y., Natural convective cooling of electronic equipment in: S. Kakac, W. Aung, R. Viskant (Eds), Natural Convection Fundamentals and Applications, Hemisphere, Washington DC, 1985.

[3] Peterson, G.P. and Ortega, A., Thermal control of electronic equipment and devices, Adv. Heat Transfer, vol. 20, pp. 281-310, 1990.

[4] Elenbaas, W., Heat Dissipation of parallel plates by free convection, Physica, vol. 9, pp. 1-28, 1942.

[5] Ostroumov, G.A., Free convection under the condition of the internal problem, NACA TM-1407, 1958.

[6] Sparrow, E.M. and Bahrami, P.A., Experiments on natural convection from vertical parallel plates with either open or closed edges, ASME. J. Heat Transfer, vol. 102, pp. 221-227, 1980.

[7] Bodoia, J.R. and Osterne, J.F., The development of free convection between heated vertical plates, ASME. J. Heat Transfer, vol. 84, pp. 40-44, 1962.

[8] Engel, R.K. and Muller, W.K, ASME paper 67-HT-16, 1967.

[9] Yao, L.S., Natural Convection along a wavy surface, ASME. J Heat Transfer, vol. 105, pp. 465-468, 1983.

[10] Yao, L.S., A note on Prandtl's transposition theorem, ASME. J Heat Transfer, vol. 110, pp. 503-507, 1988.

[11] Moulic, S.G. and Yao, L.S., Mixed convection along a wavy surface, ASME. J Heat Transfer, vol. 111, pp. 974-979, 1989.

[12] Chiu, C.P. and Chou, H.M., Transient analysis of natural convection along a vertical wavy surface in micropolar fluids, Int. J. Eng. Sci., vol. 32, pp. 19-33, 1994.

[13] Chen, C.K. and Wang, C.C., Transient analysis of force convection along a wavy surface in miropolar fluids, J. Thermophys. Heat Transfer, vol. 14, pp. 340-347, 2000.

[14] Malashetty, M.S., Umavathi, J.C. and Leela, V., Magnetoconvective flow and heat transfer between vertical wavy wall and a parallel flat wall, Int. J. Applied Mechanics and Engng. vol. 6, No.2, pp.437-456, 2001.

[15] Umavathi, J.C., Prathap-Kumar, J. and Shekar, M., Mixed convective flow of immiscible viscous fluids confined between a long vertical wavy wall and a parallel flat wall, Int. J. Eng. Sci. Tech., vol. 2, No. 6, pp. 256-277, 2010.

[16] Umavathi, J.C. and Shekar, M., Mixed convection flow and heat transfer in a vertical wavy channel containing porous and fluid layer with traveling thermal waves, Int. J. Eng. Sci. Techno., Vol. 3, No. 6, pp. 196-219, 2011.

[17] Umavathi, J.C. and Shekar, M., Mixed convective flow of two immiscible viscous fluids in a vertical wavy channel with traveling thermal waves, Heat Transfer Asian Research, vol. 40(8), pp. 721-743, 2011.

[18] Das, P.K. and Mahmud, S., Numerical investigation of natural convection inside a wavy enclosure, Int. J. Therm. Sci. vol. 42, pp. 397-406, 2003.

[19] Dalal, A. and Das, M.K., Laminar Natural convection in an inclined complicated cavity with spatially variable wall temperature, Int. J. Heat Mass Transfer, vol. 48, pp. 3833-3854, 2005.

[20] Oztop, H.F., Numerical study of flow and heat transfer in curvilinear ducts: applications of electric grid generation, Appl. Math. Comput., vol.168, pp. 1449-1460, 2005.

[21] Varon, Y. and Oztop, H.F., Effect of inclination angle on natural convection in wavy solar air collectors: A computational modeling, the 2nd International Green Energy Conference, UOIT, Oshawa, Canada, 25-29, June, 2006.

[22] Jang, J.H., Yan, W.M. and Liu, H.P., Natural convection heat and mass transfer along a vertical wavy surface, Int. J. Heat and Mass Transfer, vol. 46, pp. 1075-1083, 2003.

[23] Mahmud, S., Das, P.K., Hyder, N. and Islam, A.K.M., Free convection in an enclosure with vertical wavy wall, Int. J Thermal and Science, vol. 41, pp. 440-446, 2002.

[24] Khalil Khanafer, Baber Al-Azim, Alia Marafree, Ioan Pop, Non-Darcian effects on natural convection heat transfer in a wavy porous enclosure, Int. J. Heat Mass Transfer, vol.52, pp. 1887-1896, 2009.

[25] Hasnaoui, M., Bilgen, E. and Vasseur, P., Natural convection above an array of open cavities heated from below, Numerical Heat Transfer, vol.18, pp. 436-442, 1990.

[26] Ben-Nakhi, A. and Chamkha, A.J., Natural convection in an inclined partitioned enclosure, Int. J. Heat Mass Transfer, vol. 42, pp. 311-321, 2006.

[27] Dagtekin, I. and Oztop, H.F., Natural convection heat transfer by heated partitions within enclosures, Int. J. Heat and Mass Transfer, vol. 28, pp. 823-834, 2001.

[28] Tansmim, S.T. and Collins, M.R., Numerical analysis of heat transfer in a square cavity with a baffle on the hot wall, Int. Com. Heat Mass Transfer, vol. 31, pp. 639-650, 2004.

[29] Prathap Kumar, J., Umavathi, J.C., Ali J. Chamkha and Prema, H., Free convection in a vertical double passage wavy channel filled with a Walters fluid (model B'), Int. J. Energy & Technology, vol. 3, No. 2, pp. 1–13, 2011.

[30] Prathap Kumar, J., Umavathi, J.C. and Prema, H., Free convection of Walter's fluid flow in a vertical double-passage wavy channel with heat source, Int. J. Eng. Sci. Techno., vol. 3, No. 1, pp. 136-165, 2011.

[31] Chang, T.S. and Shiau, Y.H., Flow pulsation and baffle's effects on the opposing mixed convection in a vertical channel, Int. J. Heat and Mass Transfer, vol. 48, pp. 4190-4204, 2005.

[32] Nasiruddin and Siddiqui, M.H.K., Heat Transfer augmentation in a heat exchanger tube using a baffle, Int. J. Heat and Fluid Flow, vol. 28(2), pp. 318-328, 2007.

[33] Yang, M.H., Yeh, R.H, and Hwang, J.J., Mixed convective cooling of a fin in a channel, Int. J Heat and Mass Transfer, vol. 53(4), pp. 760-771, 2010.

[34] Cheng, C.H., Kuo, H.S., and Huang, W.H., Laminar fully developed forced-convection flow within an asymmetric heated horizontal double-passage channel, Appl. Energy, vol. 33, pp. 265-286, 1989.

[35] Salah El-Din, M.M., Fully developed laminar convection in a vertical double-passage channel, Appl. Energy, vol. 47, pp. 69-75, 1994.

[36] Salah El-Din, M.M., Effect of viscous dissipation on fully developed laminar mixed convection in a vertical double-passage channel, Int. J. Therm. Sci., vol. 41, pp. 253-259, 2002.

[37] Rita Choudhury and Alok Das, Free convection flow of a non-Newtonian fluid in a vertical channel, Defense Science Journal, vol. 50, pp. 37-44, 2000.

Source of support: Nil, Conflict of interest: None Declared

